Supporting Information

Single-molecular photosensitizers for NIR-II fluorescence and photoacoustic imaging guided precise anticancer phototherapy

Hua Gu[a], Weijian Liu[a], Wen Sun[a,b], Jianjun Du[a,b], Jiangli Fan[a,b,*], Xiaojun Peng[a]

[a] State Key Laboratory of Fine Chemicals, Dalian University of Technology, Dalian 116024, China.

[b]Ningbo Institute of Dalian University of Technology, Ningbo 315016, China.

*: Corresponding author. E-mail: fanjl@dlut.edu.cn.

4. Experiential Section

Materials

The chemical intermediates of 5-formylthiophen-2-boronic acid, tributyl(thiophen-2-yl) stannane, 4-bromo-4,4-dimethyltriphenylamine, palladium catalyst, piperidine, 7-bromobenzo[c][1,2,5]thiadiazole-4-carbaldehyde, phosphorus oxychloride, 3,(4,5-dimethylthiazol-2-yl)-2,5-diphenyl tetrazolium bromide (MTT), and 9,10-anthracenyl-bis(methylene)-dimalonic acid (ABDA) were commercially available. The solvents were ordered from Xilong Scientific and Damao Chemical Reagent. Dulbecco's modified eagle medium (DMEM), phosphate-buffered saline (PBS), fetal bovine serum (FBS), penicillin, and streptomycin (P/S) were purchased from Beijing Solarbio Science & Technology Co., Ltd; Reactive oxygen species assay kit (DCFH-DA), calcein AM/propidium (AM/PI) and mitochondrial-blue tracker (Mito-blue) were purchased from Keygen Biotechnology.

This study was conducted in accordance with the Guide for the Care and Use of Laboratory Animals published by the US National Institutes of Health (8th edition, 2011). The animal protocol was approved by the local research ethics review board of the Animal Ethics Committee of Dalian University of Technology.

sm-PSs synthesis

7-(5-(4-(di-p-tolylamino)phenyl)thiophen-2-yl)benzo[c][1,2,5]thiadiazole-4-carbaldehyde (BTT-CHO): in a 50-mL flask, ThMeTPA (0.38 g, 1 mmol) was dissolved in 20 mL THF (extra dry) at -80 °C under N_2 atmosphere. n-BuLi (7.5 mL, 1.2 mmol, 1.6 M in hexane) was added dropwise, and the mixture was stirred for 2 h. Next, tributyltin chloride (0.39 g, 1.2 mmol) was added dropwise, and the mixture was stirred for another 6 h. The reaction solution was extracted with ethyl acetate, washed with water, and dried over magnesium sulfate. A rotary evaporator concentrated the mixture without further purification for the next reaction. The stannide (1.6 g, 2.5 mmol), 7-bromobenzo[c][1,2,5]thiadiazole-4-carbaldehyde (0.24 g, 1 mmol), and $Pd(dppf)_2Cl_2$ (0.035 g, 0.05 mmol) were dissolved in 20 mL toluene under N_2 atmosphere. The mixture was refluxed for 12 h. Then, the reaction was cooled to room temperature, poured into 50 mL water, and then extracted with ethyl acetate. The extract liquor was washed with water and dried over with magnesium sulfate. The mixture was concentrated by a rotary evaporator, and the target molecular was purified via a silica gel column (PE: CH_2Cl_2 = 3:1). ^1H NMR (400 MHz,

DMSO) δ 10.62 (s, 1H), 8.37 (d, J = 4.0 Hz, 1H), 8.35 – 8.30 (m, 2H), 7.68 (d, J = 8.7 Hz, 2H), 7.62 (d, J = 4.1 Hz, 1H), 7.18 (d, J = 8.1 Hz, 4H), 7.01 (d, J = 8.3 Hz, 4H), 6.95 (d, J = 8.7 Hz, 2H), 2.31 (s, 6H). ^{13}C NMR (101 MHz, DMSO) δ 189.95 (s), 155.47 (s), 152.27 (s), 148.80 (s), 144.64 (s), 143.47 – 143.27 (m), 134.24 (s), 133.58 (d, J = 3.0 Hz), 130.70 (s), 129.92 (s), 127.96 (d, J = 5.8 Hz), 127.72 (s), 127.08 (s), 125.45 (d, J = 0.4 Hz), 121.56 (s), 20.92 (s). MALDI-TOF MASS calculated m/z for [$C_{31}H_{23}N_3OS_2$] calculated 517.1277, found (m/z): 517.1291.

(E)-4-(5-(2-(1,1-dimethyl-3-propyl-1H-3l4-benzo[e]indol-2-yl)vinyl)thiophen-2-yl)-N,N-di-p-tolylaniline (CyE-TT), **(E)-4-(5-(2-(1,1-dimethyl-3-(3-(trimethyl-l4-azaneyl)propyl)-1H-3l4-benzo[e]indol-2-yl)vinyl)thiophen-2-yl)-N,N-di-p-tolylaniline (CyQN-TT)** and **(E)-4-(5-(7-(2-(1,1-dimethyl-3-(3-(trimethyl-l4-azaneyl)propyl)-1H-3,4-benzo[e]indol-2-yl)vinyl)benzo[c][1,2,5]thiadiazol-4-yl)thiophen-2-yl)-N,N-di-p-tolylaniline (CyQN-BTT)** have the same reaction conditions and processes: CyE/CyQN (1.2 mmol) and TT-CHO/BTT-CHO (1 mmol) were added to a 50-mL flask with 22 mL ethanol under N_2 atmosphere. While stirring, piperidine (0.2 mL) was added. The mixture was stirred at 78 ℃ for 6 h and stopped. When the mixture was cooled down to room temperature, 50 mL diethyl ether was added. The precipitate was filtered and washed three times with ether and ethyl acetate. The target molecules were obtained via further refinement with neutral silicone.

CyE-TT: Black solid with yield of 68%. ^{1}H NMR (400 MHz, DMSO) δ 8.76 (d, J = 15.8 Hz, 1H), 8.42 (d, J = 8.4 Hz, 1H), 8.28 (d, J = 9.0 Hz, 1H), 8.23 – 8.19 (m, 2H), 8.08 (d, J = 9.0 Hz, 1H), 7.79 (dd, J = 16.1, 7.8 Hz, 2H), 7.71 (dd, J = 10.1, 6.3 Hz, 4H), 7.20 (d, J = 8.3 Hz, 5H), 7.04 (d, J = 8.3 Hz, 4H), 6.92 (d, J = 8.8 Hz, 2H), 4.75 (d, J = 7.1 Hz, 2H), 2.31 (s, 6H), 2.02 (s, 6H), 1.49 (t, J = 7.2 Hz, 3H). ^{13}C NMR (400 MHz, CD_3OD) δ 155.02 (s), 149.83 (s), 145.47 (s), 144.15 (s), 138.62 (d, J = 15.8 Hz), 138.32 (s), 134.32 (s), 133.42 (s), 130.83 (s), 128.84 (s), 127.85 (s), 127.35 (s), 126.02 (s), 124.84 (s), 120.48 (s), 113.35 (s), 108.66 (s), 55.39 (s), 53.80 (s), 26.16 (s), 20.96 (s), 14.20 (s). MALDI-TOF MASS calculated m/z for $[C_{42}H_{39}N_2S]^+$ calculated 603.2828, found (m/z): 603.2808.

CyQN-TT: Black solid with yield of 72%. ^{1}H NMR (400 MHz, DMSO) δ 8.76 (d, J = 15.8 Hz, 1H), 8.42 (d, J = 8.4 Hz, 1H), 8.28 (d, J = 9.0 Hz, 1H), 8.23 – 8.19 (m, 2H), 8.08 (d, J = 9.0 Hz, 1H), 7.79 (dd, J = 16.1, 7.8 Hz, 2H), 7.71 (dd, J = 10.1, 6.3 Hz, 4H), 7.20 (d, J = 8.3 Hz, 5H), 7.04 (d, J = 8.3 Hz, 4H), 6.92 (d, J = 8.8 Hz, 2H), 4.75 (d, J = 7.1 Hz, 2H), 2.31 (s, 6H), 2.02 (s,

6H), 1.49 (t, *J* = 7.2 Hz, 3H). ^{13}C NMR (400 MHz, CD_3OD) δ 181.75 (s), 157.88 (s), 150.46 (s), 146.36 (s), 144.00 (s), 138.21 (d, *J* = 10.1 Hz), 137.74 (s), 134.35 (s), 133.61 (s), 131.40 (s), 129.92 (d, *J* = 4.6 Hz), 128.18 (s), 127.36 (d, *J* = 10.6 Hz), 126.84 (s), 125.60 (s), 124.71 (s), 124.40 (s), 122.61 (s), 119.83 (s), 111.88 (s), 107.02 (s), 62.67 (s), 53.65 (s), 52.60 (s), 25.59 (s), 22.11 (s), 19.46 (s). High-resolution mass spectra calculated m/z for $[C_{46}H_{49}N_3S]^{2+}$ calculated 337.6818, found (m/z): 337.6822.

CyQN-BTT: Black solid with yield of 46%. ^{1}H NMR (400 MHz, DMSO) *δ* 8.94 (d, *J* = 16.0 Hz, 1H), 8.76 (t, *J* = 15.4 Hz, 2H), 8.52 (d, *J* = 8.3 Hz, 1H), 8.46 (d, *J* = 3.9 Hz, 1H), 8.43 – 8.35 (m, 2H), 8.33 – 8.25 (m, 2H), 7.86 (t, *J* = 7.6 Hz, 1H), 7.81 – 7.76 (m, 1H), 7.68 (t, *J* = 6.6 Hz, 3H), 7.18 (d, *J* = 8.2 Hz, 4H), 7.01 (d, *J* = 8.3 Hz, 4H), 6.95 (d, *J* = 8.6 Hz, 2H), 4.87 (s, 2H), 3.82 (s, 2H), 3.15 (s, 9H), 3.08 (s, 2H), 2.30 (s, 6H), 2.15 (s, 6H). High-resolution mass spectra calculated m/z for $[M\text{-}2Br]^{2+}$calcd for $C_{52}H_{51}N_5S_2$, 404.6788; found, 404.6788.

Fourier transform infrared (FT-IR) spectra experiment

Three molecules were ground into powder and mixed with anhydrous potassium bromide in a ratio of 1.0 mg (sample) to 100.0 mg (anhydrous potassium bromide), respectively. A tablet press was used to press the mixed solid powder into 1~2 mm thick slices. The FT-IR absorption spectra was tested and recorded with Bruker Vertex 70 FT-IR (Bruck, MPA, Germany), as shown in Fig. S18. And the FT-IR absorption peak assignment was also listed in Table S1.

Melting point test

Melting point (m.p.) was tested via Differential scanning calorimetry (DSC; Differential Scanning Microcalorimeter, TA Instruments, Nano DSC, America). DSC measurements were carried out with ~3 mg samples at a heating rate of 10 °C min-1 and a cooling rate of 25 °C min-1 in the temperature range of 40 to 200 °C.

PCE calculation

The detailed PCE calculation method was based on our previous work.[1] All conditions were consistent except for a small number of distinguishing variables. In this study, the sm-PSs (1.5 mL, 50 μg mL^{-1}) were irradiated under a 671-nm laser (0.4 W cm^{-2}) for 10 min.

Intracellular uptake and colocalization

To trace the cell-entry time and intracellular organelle localization, sm-PSs (10.0 μL, 1.0 mg

mL^{-1}) was added to cancer cells (MCF-7 and HepG2) and normal cells (3T3 and 1064) for coincubation (cell concentration: 10^6 / mL), respectively. First, the intracellular fluorescence was monitored by a confocal laser scanning microscope (CLSM, Olympus FV3000). When the intracellular brightness became the highest, the Mito-green tracker was added and coincubated for 30 min. Then, the targeting ability of sm-PSs was studied and evaluated via CLSM.

$^1O_2$ detection

ABDA was selected as the probe to detect $^1O_2$ generation in PBS. Briefly, the mixtures of ABDA and sm-PSs in PBS were irradiated under a 671-nm laser (10.0 mW cm^{-2}). The degradation of absorbance of ABDA was recorded by a UV–vis–NIR spectrophotometer. In addition, DCFH-DA was chosen as an intracellular ROS indicator. First, MCF-7 cells (cell concentration: 10^6 / mL) and sm-PSs (10.0 μL, 1.0 mg mL^{-1}) were coincubated for 24 h in the dark. Then, DCFH-DA (5.0 μL) was added. After 20 min coincubation, the experimental groups were irradiated under a 671-nm laser (10.0 mW cm^{-2}) for 2 min. After another 30 min of coincubation, the fluorescence signal was monitored by CLSM. Finally, the control group images were obtained under the same conditions except for variables.

In vitro cytotoxicity

In our previous work, we verified the phototoxicity and dark toxicity of sm-PSs for 4T1 and 3T3 cells (cell concentration: 10^6 / mL), respectively. Briefly, Calcein-AM/PI (5.0 μL) was added to four groups of 4T1 or 3T3 cells treated by PBS, PBS + laser, sm-PSs (10.0 μL, 1.0 mg mL^{-1}), and sm-PSs (10.0 μL, 1.0 mg mL^{-1}) + laser, respectively. The final staining results were recorded by CLSM. Next, we replaced Calcein-AM/PI with MTT (0.5 mg mL^{-1}) following the above procedure. Finally, the resulting formazan compound was dissolved by DMSO, and its optical absorption was detected in an enzyme-labeled instrument. Furthermore, because CyQN-BTT has both PDT and PTT abilities, two additional control groups were added, Vitamin C (VC) to consume ROS and low-power irradiation (0.1 W cm^{-2}) variables to prevent light-to-heat conversion.

Tumor-bearing mouse model

All in vivo studies were approved by the Dalian Medical University Animal Care and Use Committee. A total of 150.0 μL of 4T1 cells (1×10^7 / mL) in PBS was inoculated in the underarm epidermis of mice (BALB/c, female, 4 weeks of age, Jilin Changsheng Biotechnology). When the tumor reached ~100 mm^3 in size, these mice were used directly for bioimaging and phototherapy.

Multi-model bioimaging

We injected 100.0 μL of CyQN-BTT (1.0 mg mL^{-1}) through a mouse tail vein until the tumor reached 100 mm^3 in size. The NIR-II FLI (Ex: 800 nm, Em: 900-1100 nm, exposure time: 300 ms; NIR-II Fluorescence In Vivo Imaging System, Series III 900/1700), PAI (PST-PAFT, America), and PTI (laser: 671 nm, 0.4 W cm^{-2}, FLIR camera, 1910582) were performed to explore the enriched time in the tumor site.

In vivo antitumor efficiency

One phototherapy group and three control groups were established containing five tumor-bearing mice. Each mouse was injected with CyQN-BTT (100.0 μL, 1.0 mg mL^{-1}) in a tail vein. The tumor-bearing mice in the phototherapy group were exposed to the 671-nm laser (0.4 W cm^{-2}) for 10 min. The other three control groups were treated with PBS only, PBS + laser, and CyQN-BTT only, respectively. The tumor size and bodyweight of all the mice were monitored every 3 days until 15 days had passed. Eventually, all the mice were euthanized, and their primary organs and tumors were collected to assess the biosafety of sm-PSs.

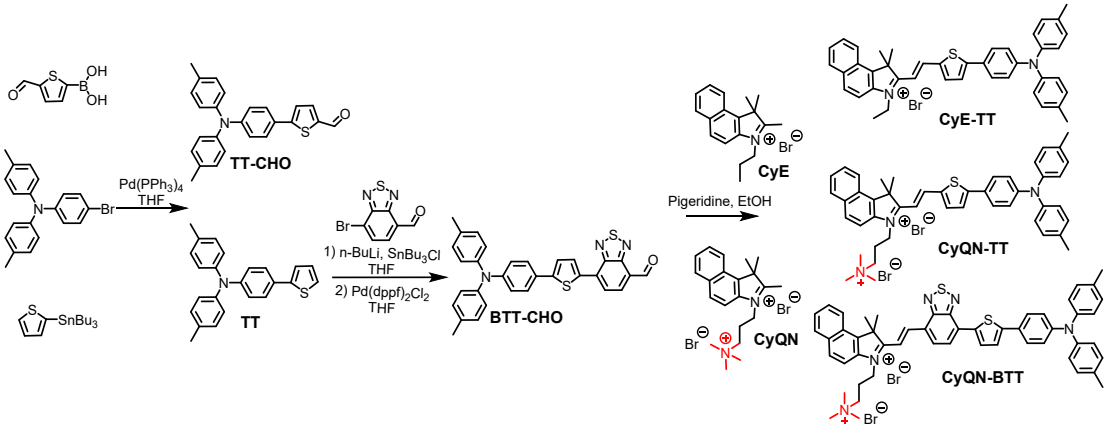

Fig. S1 Synthetic route of target AIEgens.

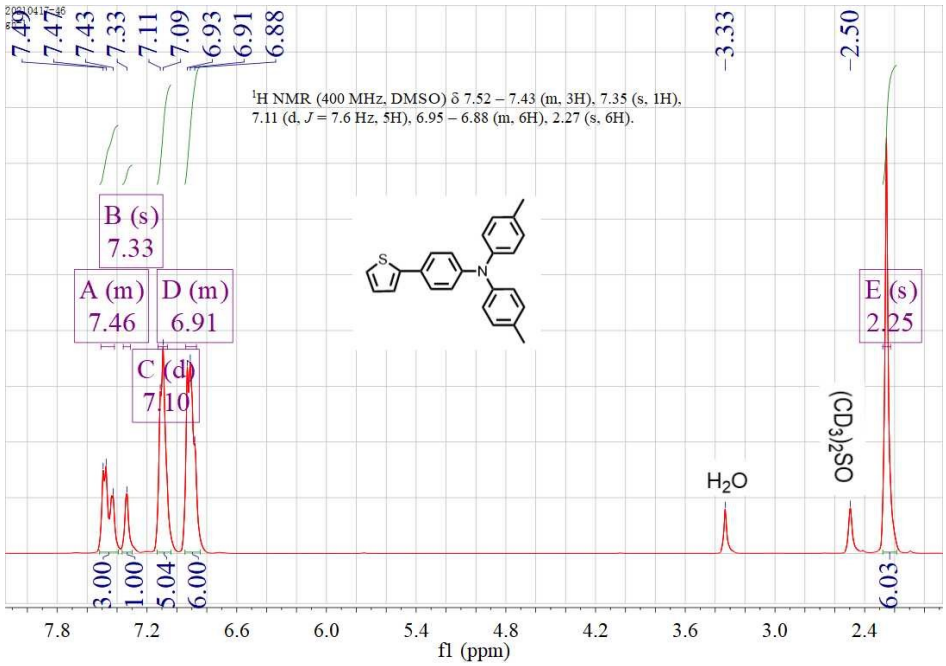

Fig. S2 ^{1}H of TT in DMSO-d_6.

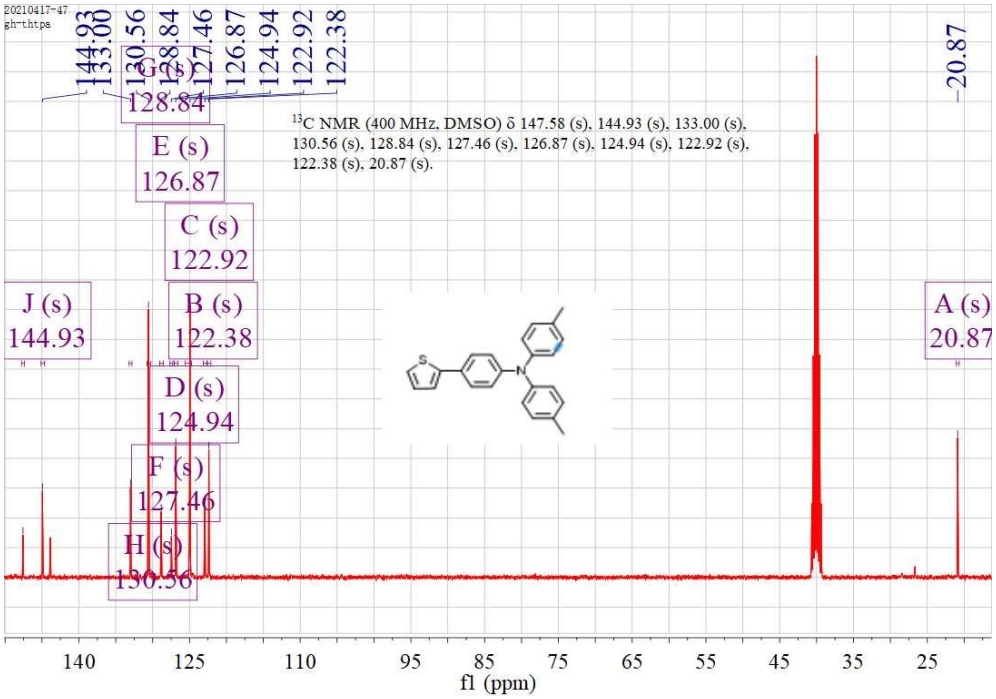

Fig. S3 ^{13}C of TT in DMSO-d_6.

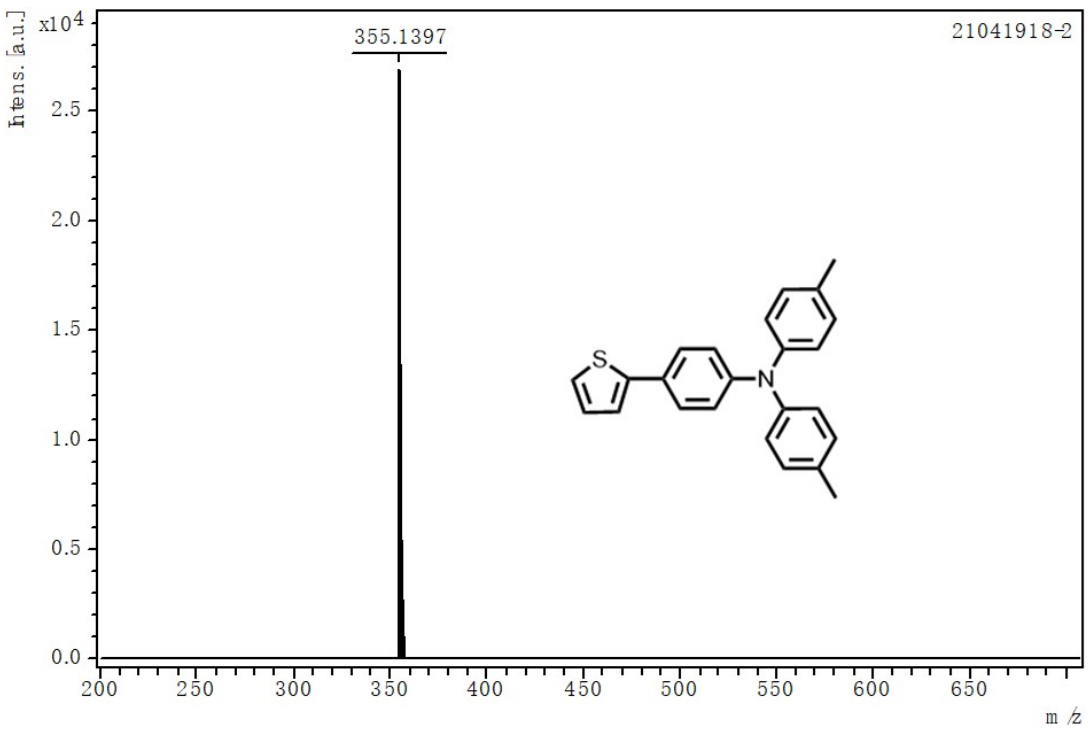

Fig. S4 The high-resolution mass spectra of TT.

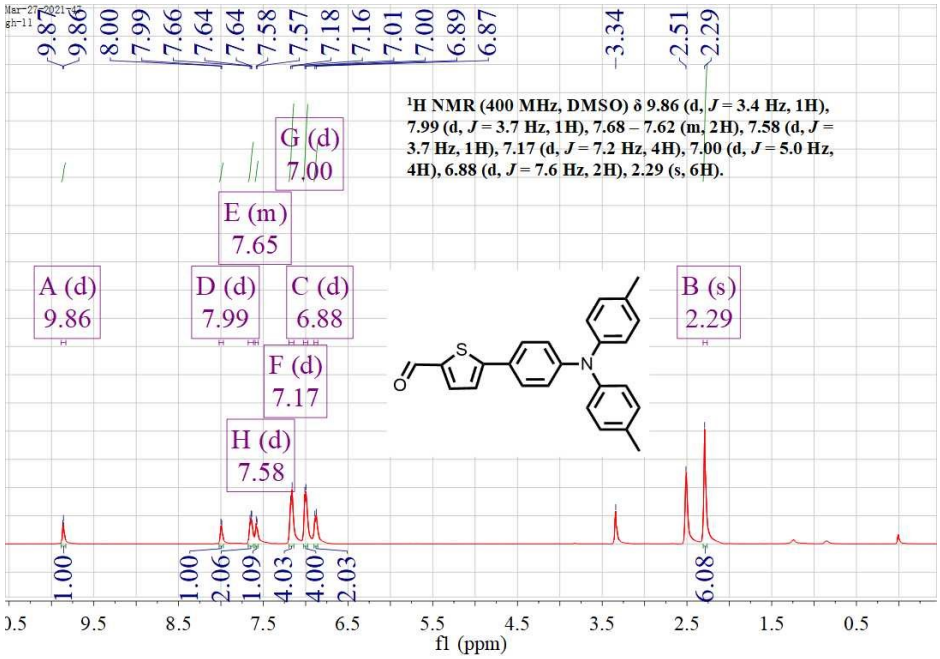

Fig. S5 ^{1}H of TT-CHO in DMSO-d_6.

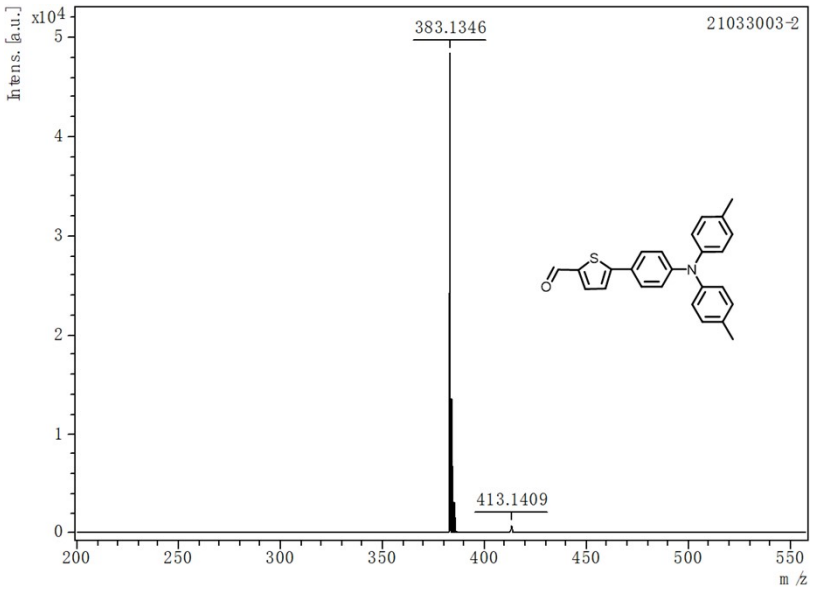

Fig. S6 The high-resolution mass spectra of TT-CHO.

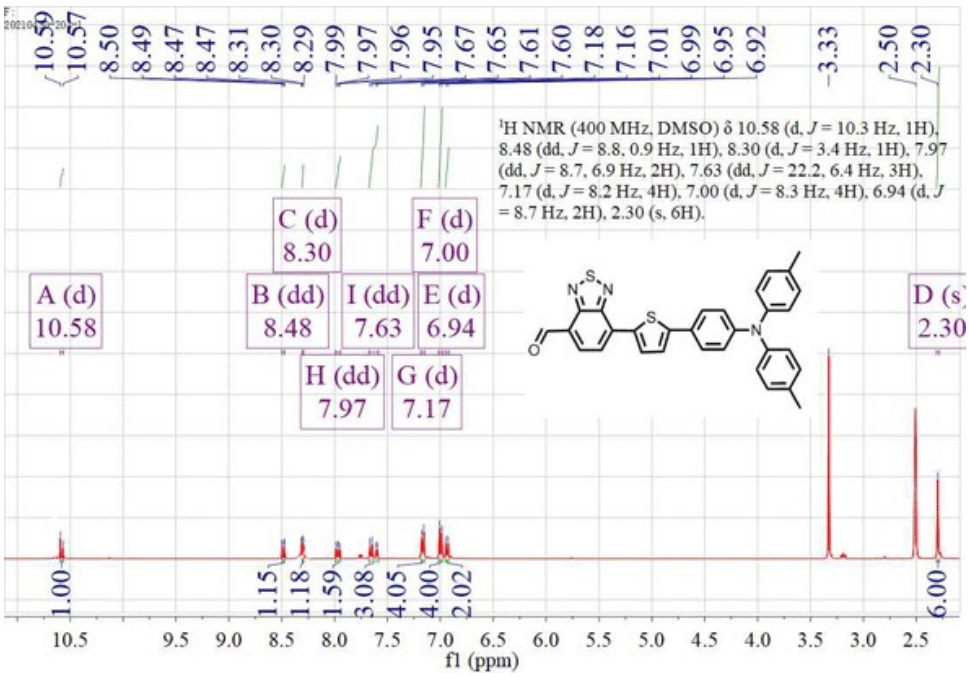

Fig. S7 ^{1}H of BTT-CHO in DMSO-d_6.

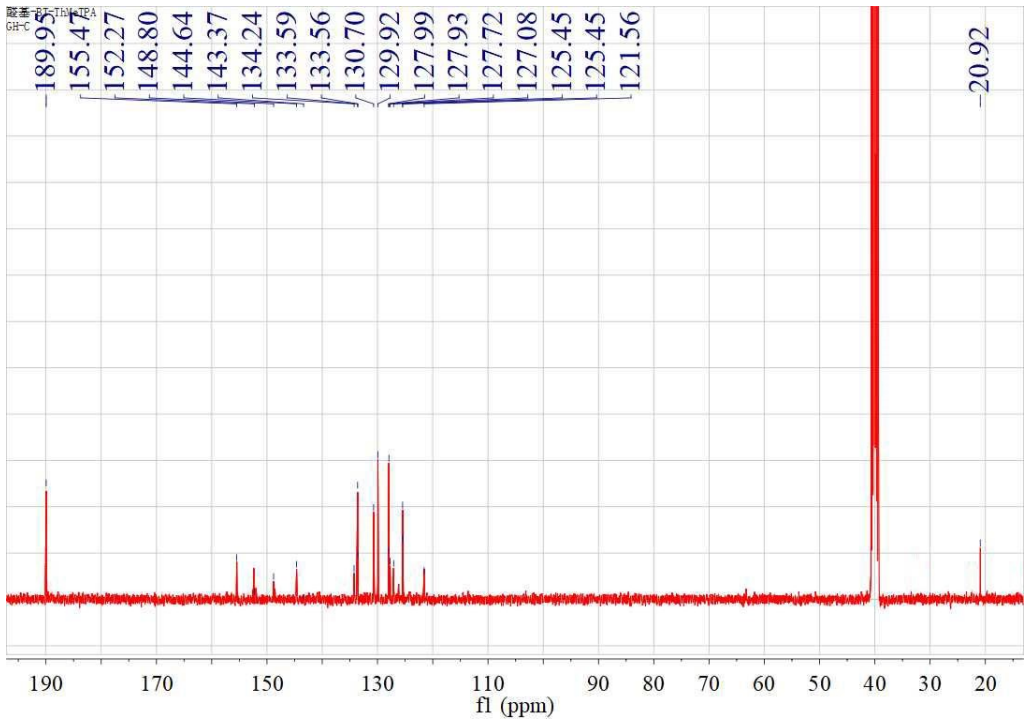

Fig. S8 ^{13}C of BTT-CHO in DMSO-d_6.

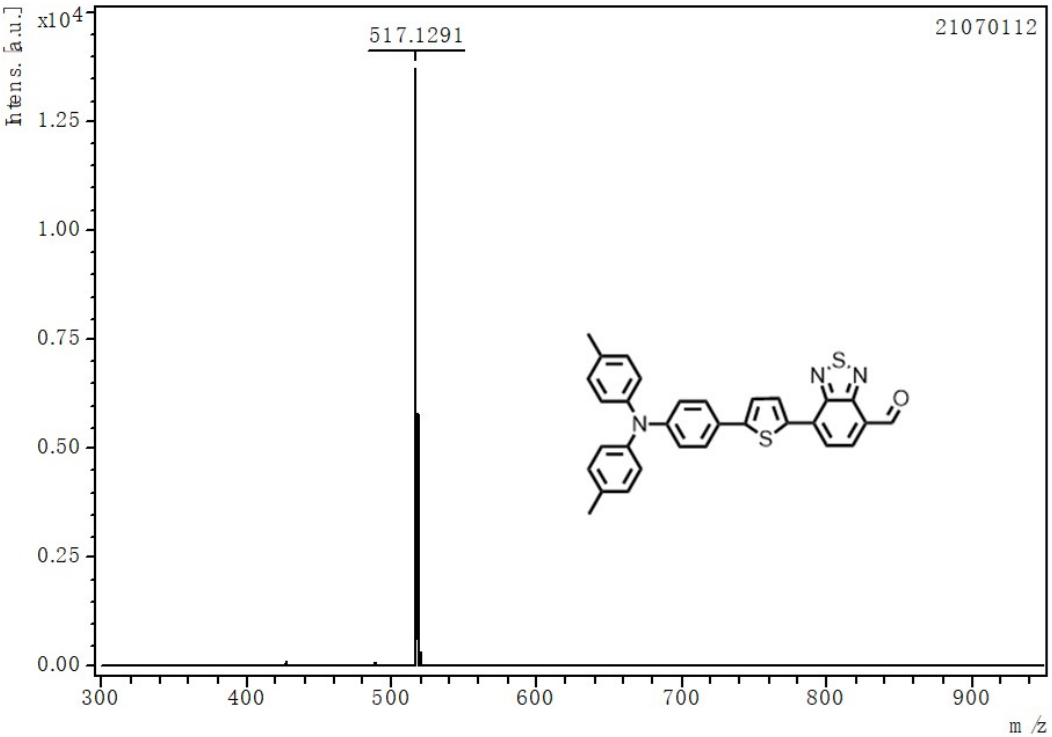

Fig. S9 The high-resolution mass spectra of BTT-CHO

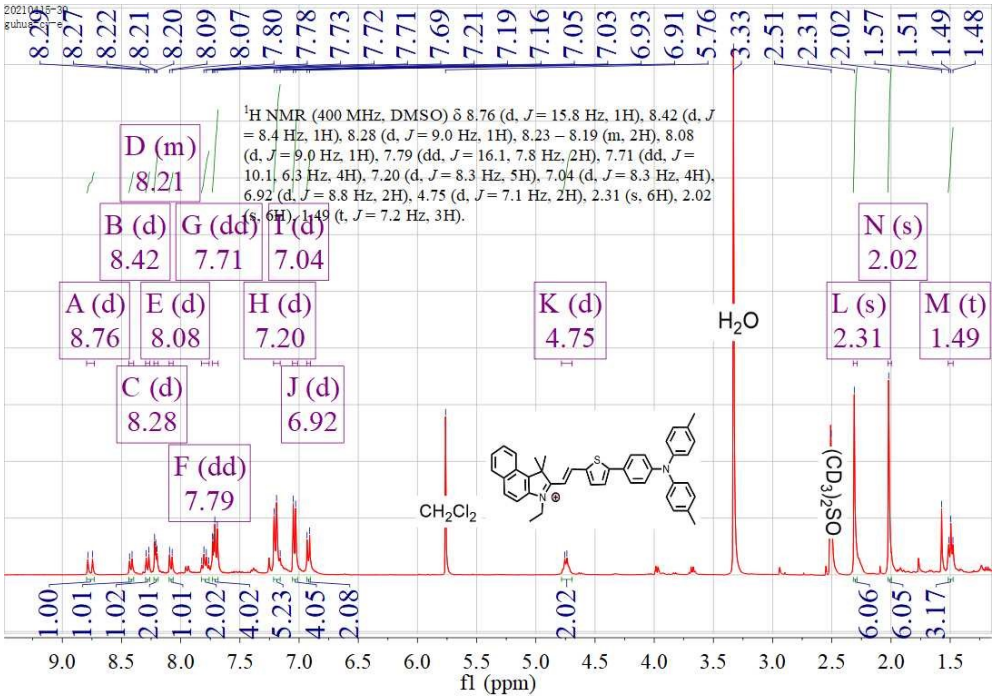

Fig. S10 ^{1}H of CyE-TT in DMSO-d_6.

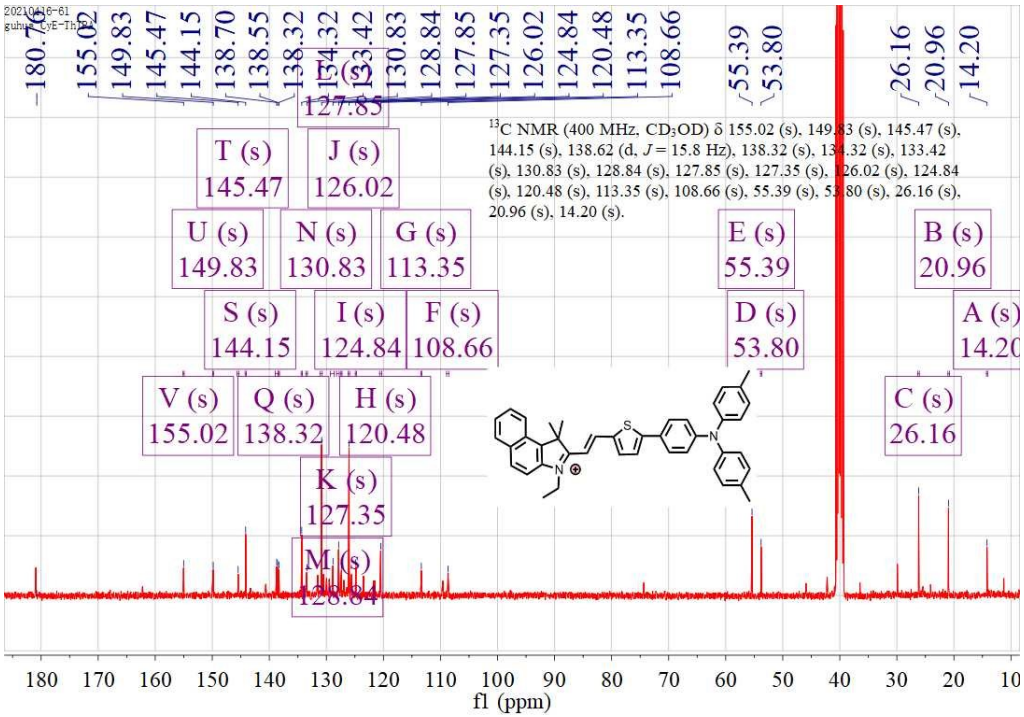

Fig. S11 ^{13}C of CyE-TT in DMSO-d_6.

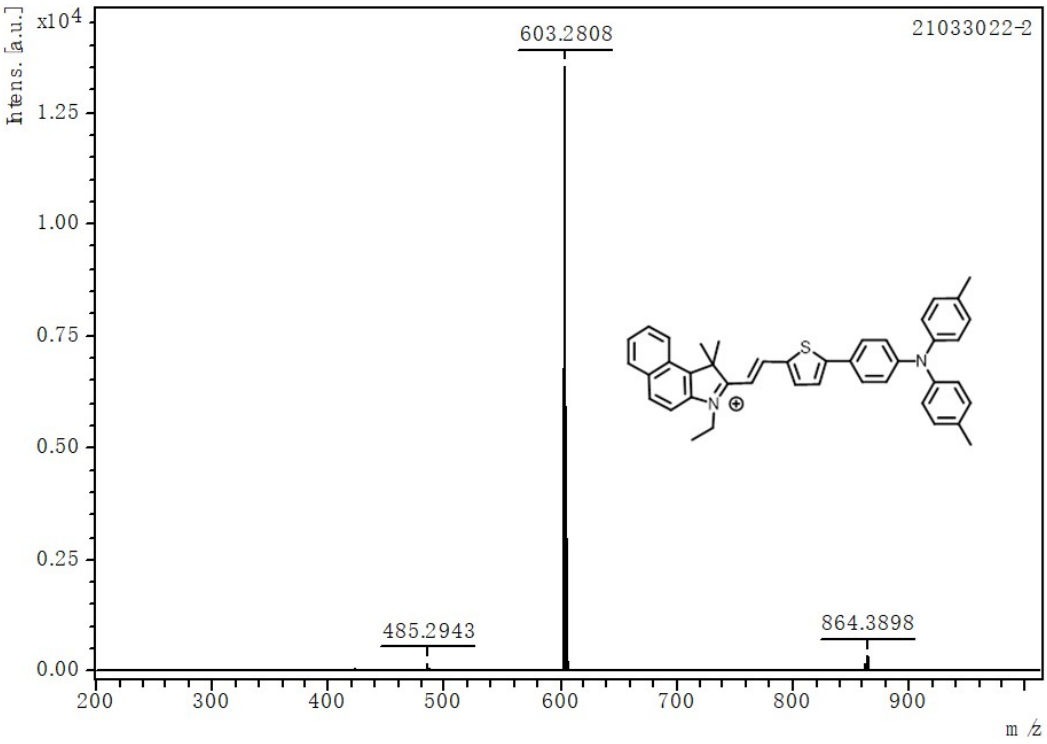

Fig. S12 The high-resolution mass spectra of **CyE-TT**

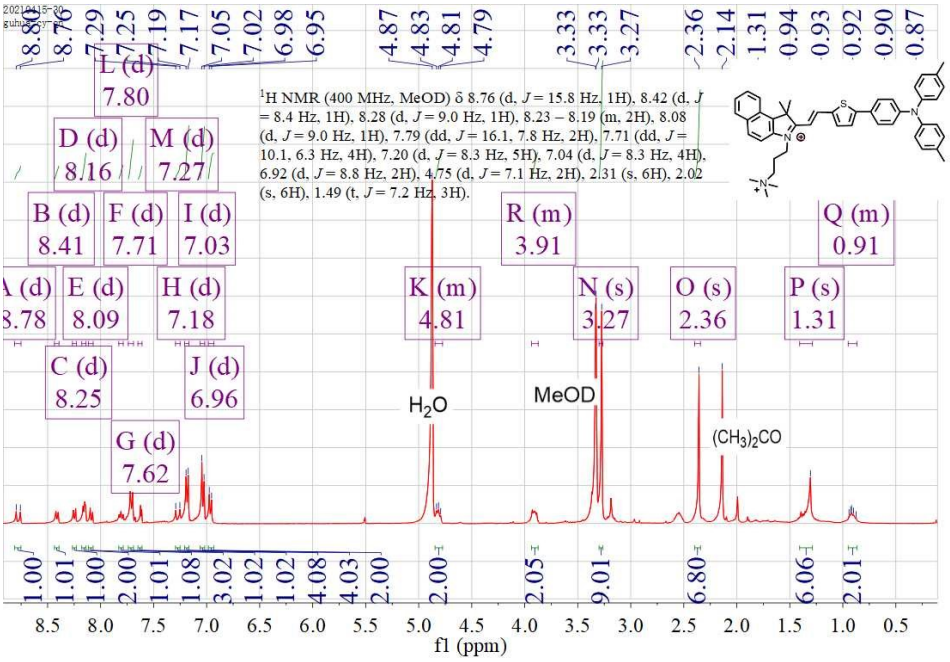

Fig. S13 ^{13}C of CyQN-TT in MeOD.

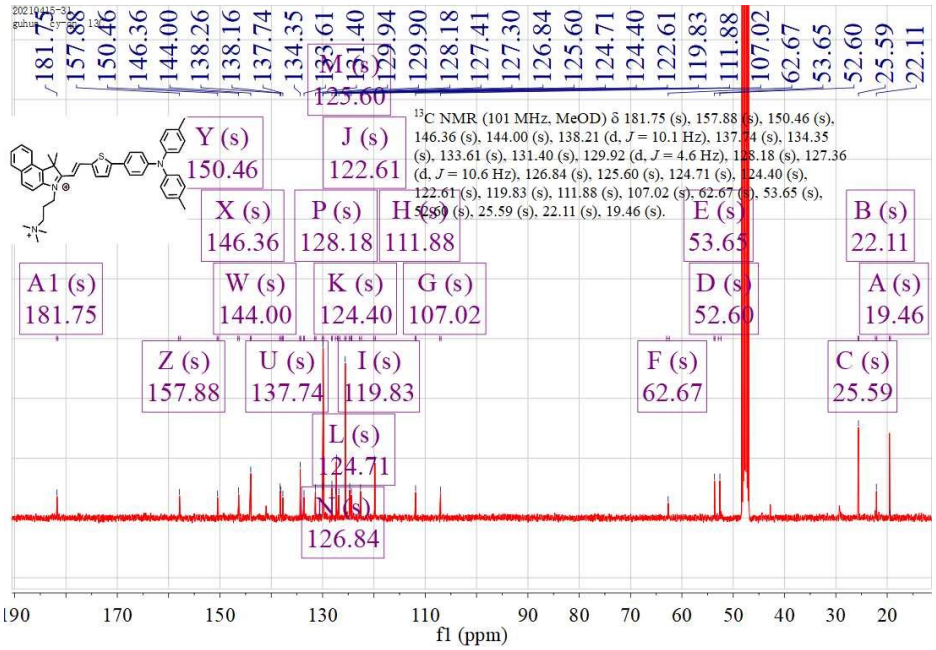

Fig. S14 ^{13}C of CyQN-TT in MeOD.

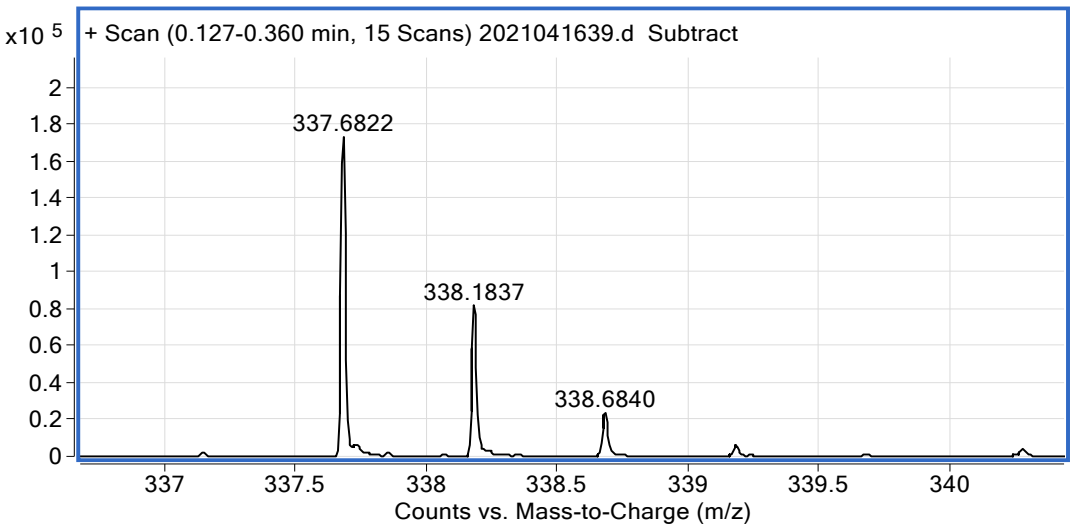

Fig. S15 **The high-resolution mass spectra of CyQN-TT**

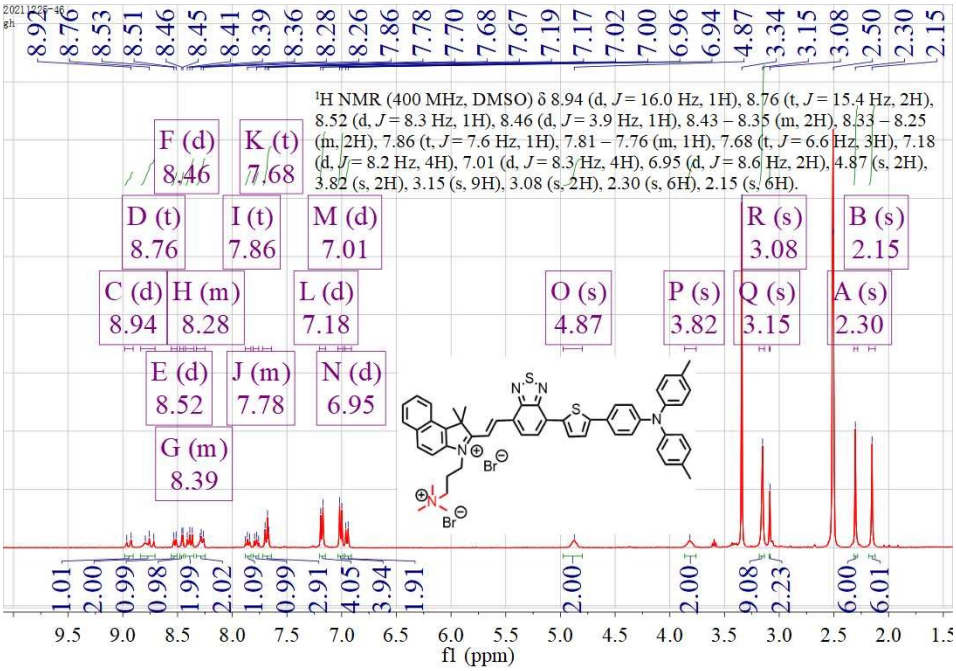

Fig. S16 ^{1}H of CyQN-BTT in DMSO-d_6.

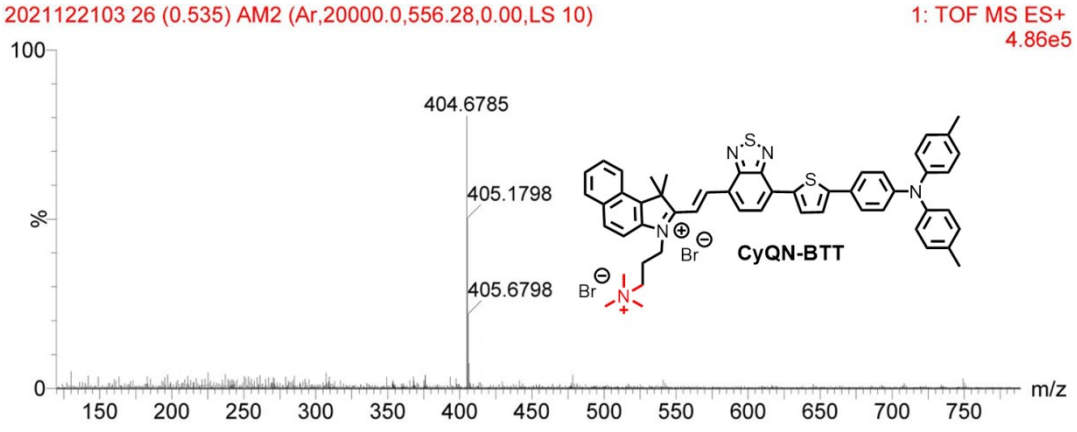

Fig. S17 The high-resolution mass spectra of CyQN-BTT

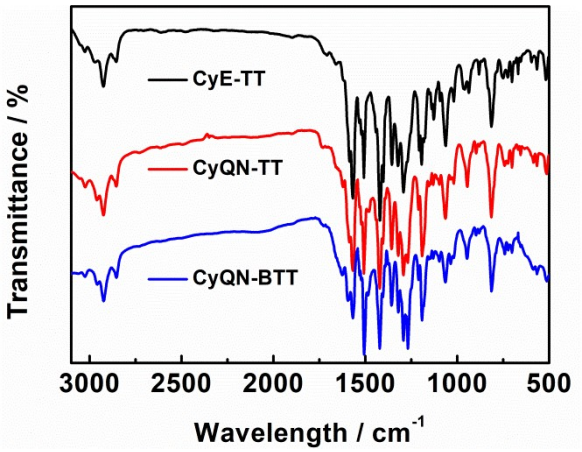

Fig. S18 FT-IR apectra of CyE-TT, CyQN-TT, and CyQN-BTT.

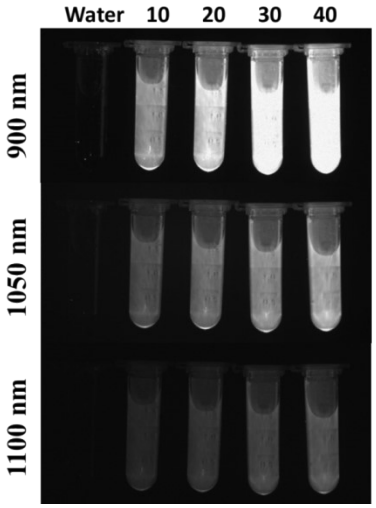

Fig. S19 The fluorescence intensity of CyQN-BTT in PBS with different concentrations under different filters. (Ex: 800 nm, Em: 900-1100 nm, exposure time: 300 ms)

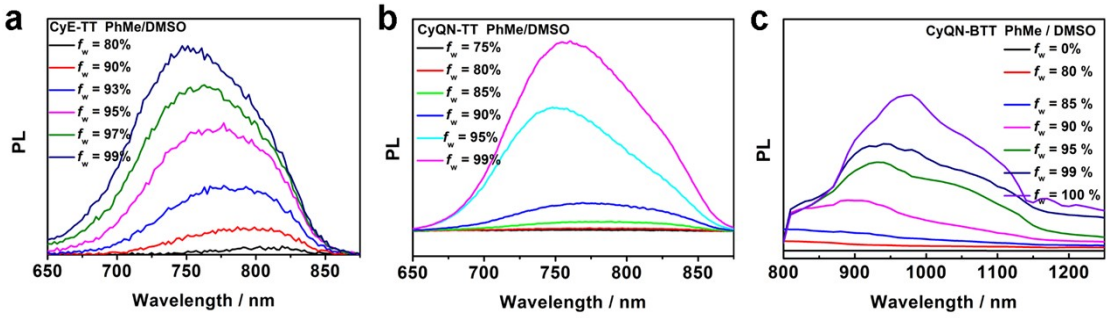

Fig. S20 the FL feature of CyE-TT, CyQN-TT, and CyQN-BTT using PhMe/DMSO mixtures with different toluene fractions (f_w) as solvent.

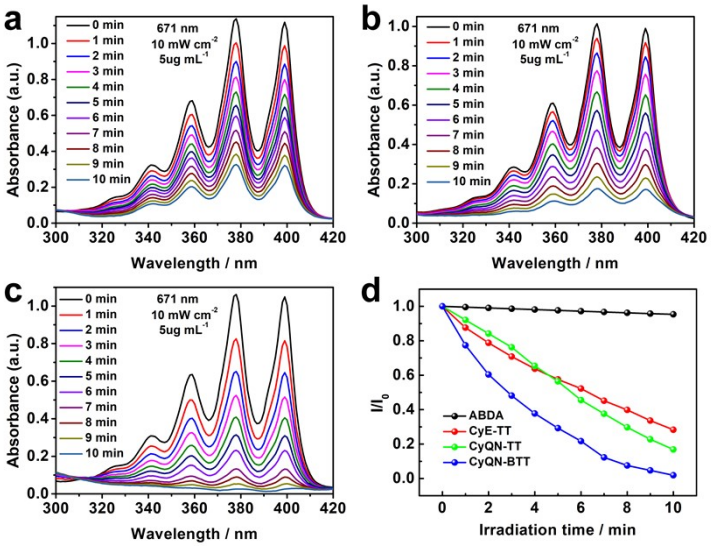

Fig. S21 The $^1O_2$ generation of CyE-TT, CyQN-TT and CyQN-BTT with ABDA as a probe in PBS under 671 nm laser (10 mW cm^{-2}).

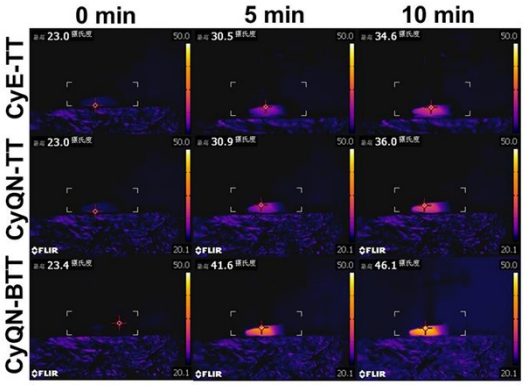

Fig. S22 The temperature changes of CyE-TT, CyQN-TT and CyQN-BTT under 671 nm laser (0.4 W cm^{-2}) with different time (50 μg mL^{-1}).

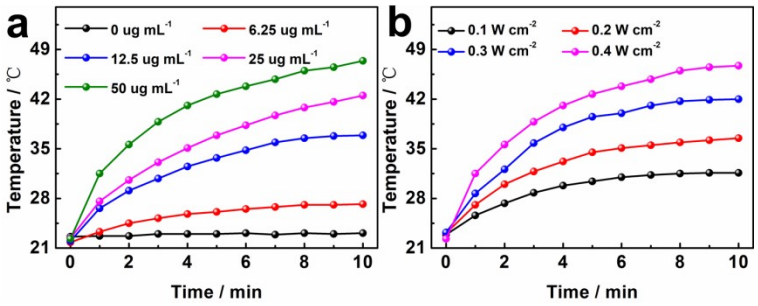

Fig. S23 The photothermal conversion behaviors of CyQN-BTT under 671 nm irradiation with different concentrations and laser power.

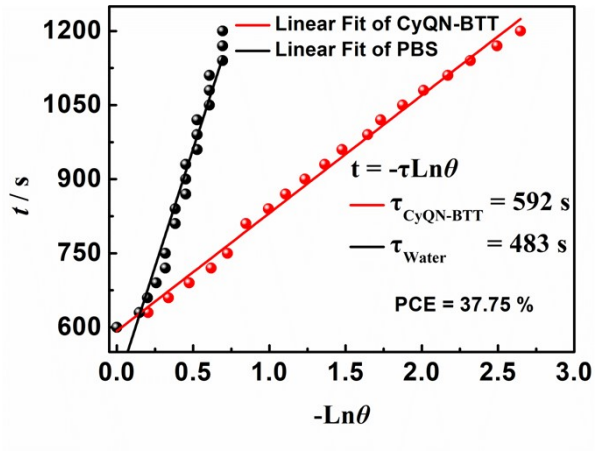

Fig. S24 The time constant for CyQN-BTT and PBS heat transfer from the system.

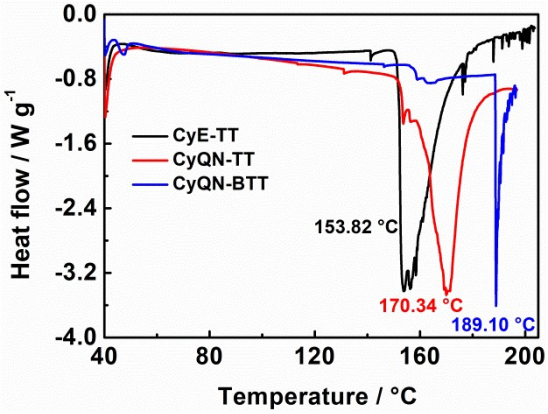

Fig. S25 Melting point apectra of CyE-TT, CyQN-TT, and CyQN-BTT.

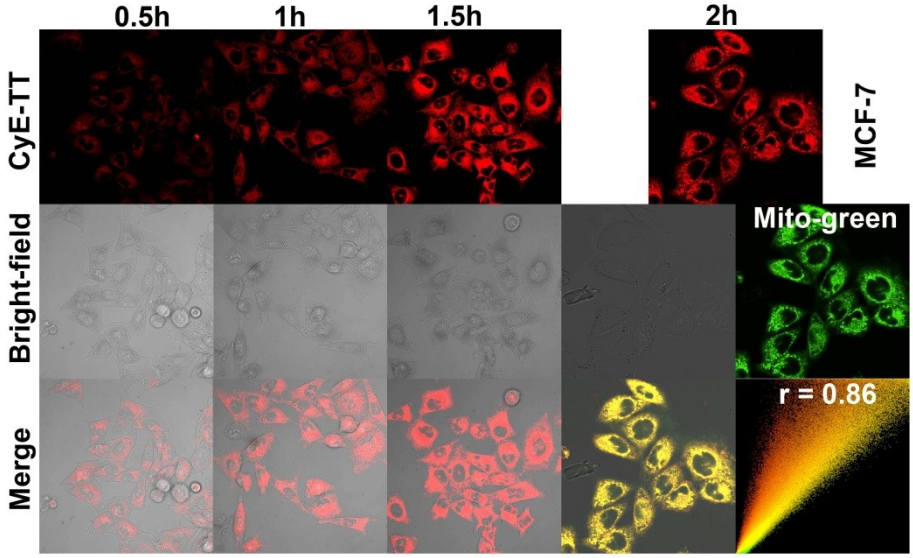

Fig. S26 The intracellular uptake and co-localization CLSM images of CyE-TT in MCF-7 cells. (scale bar: 20.0 μm)

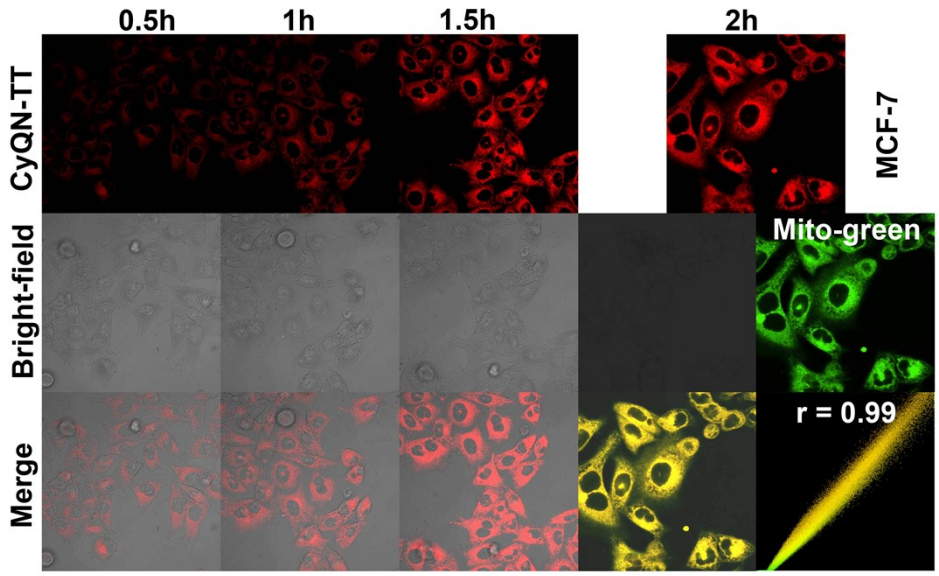

Fig. S27 The intracellular uptake and co-localization CLSM images of CyQN-TT in MCF-7 cells. (scale bar: 20.0 μm)

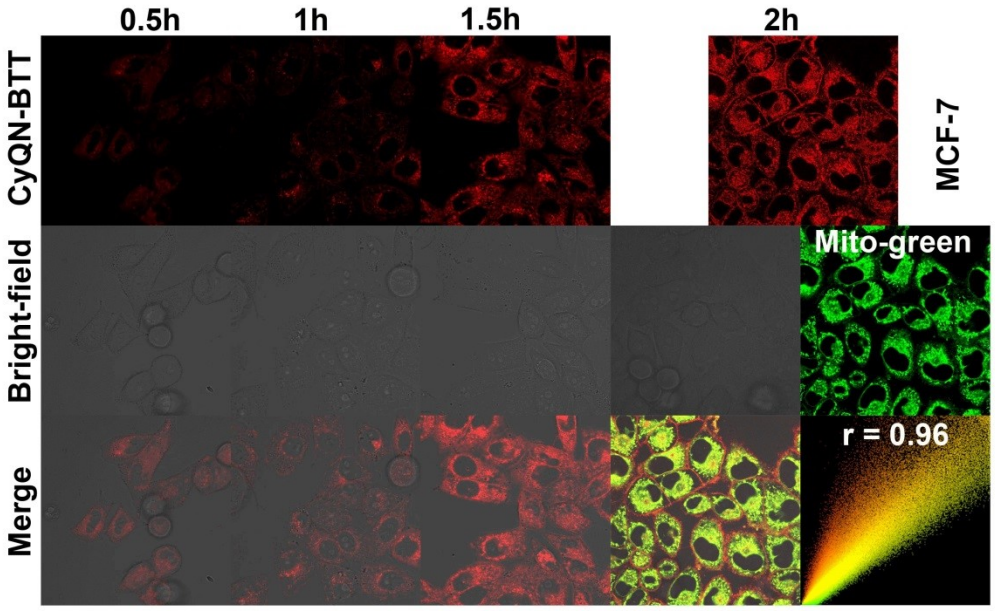

Fig. S28 The intracellular uptake and co-localization CLSM images of CyQN-BTT in MCF-7 cells. (scale bar: 20.0 μm)

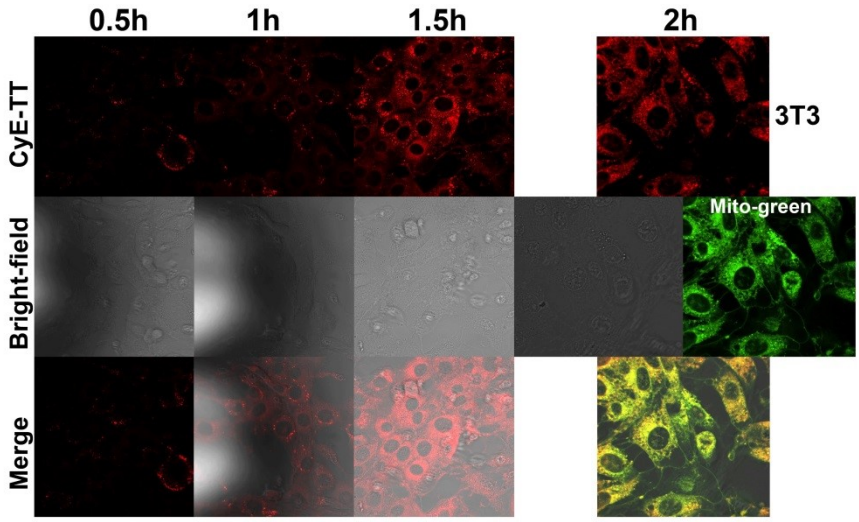

Fig. S29 The intracellular uptake and co-localization CLSM images of CyE-TT in 3T3 cells. (scale bar: 20.0 μm)

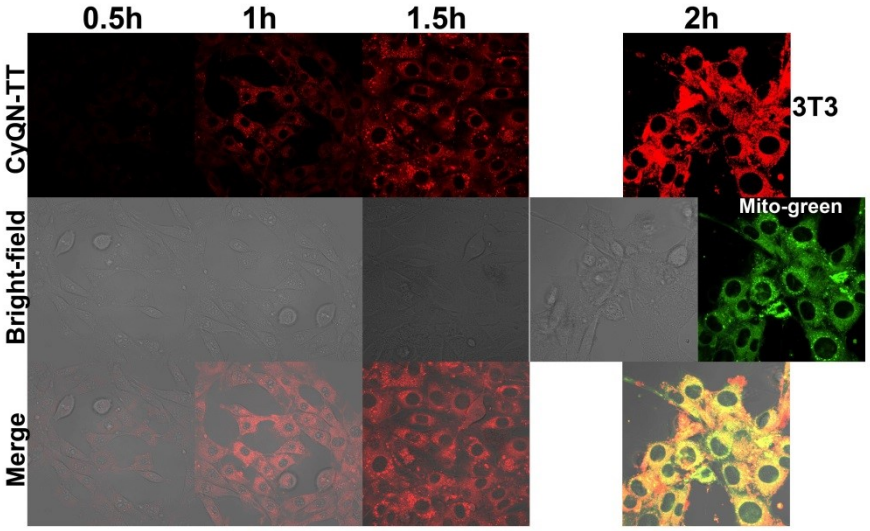

Fig. S30 The intracellular uptake and co-localization CLSM images of CyQN-TT in 3T3 cells. (scale bar: 20.0 μm)

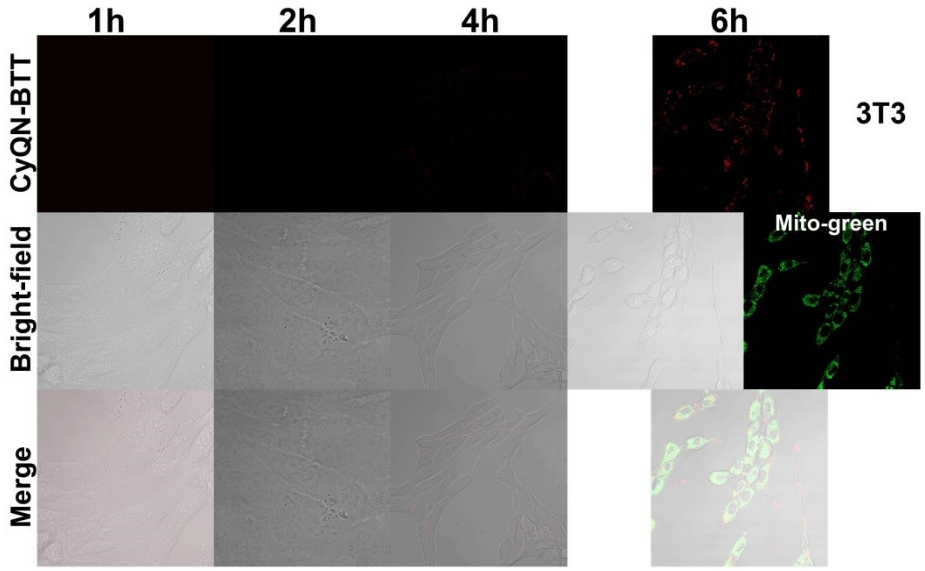

Fig. S31 The intracellular uptake and co-localization CLSM images of CyQN-BTT in 3T3 cells. (scale bar: 50.0 μm)

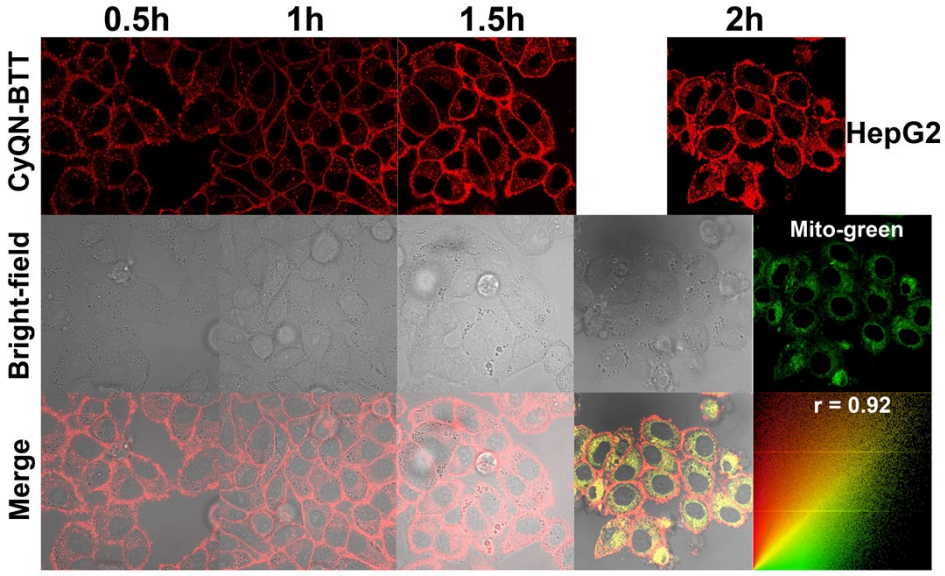

Fig. S32 The intracellular uptake and co-localization CLSM images of CyQN-BTT in HepG2 cells. (scale bar: 20.0 μm)

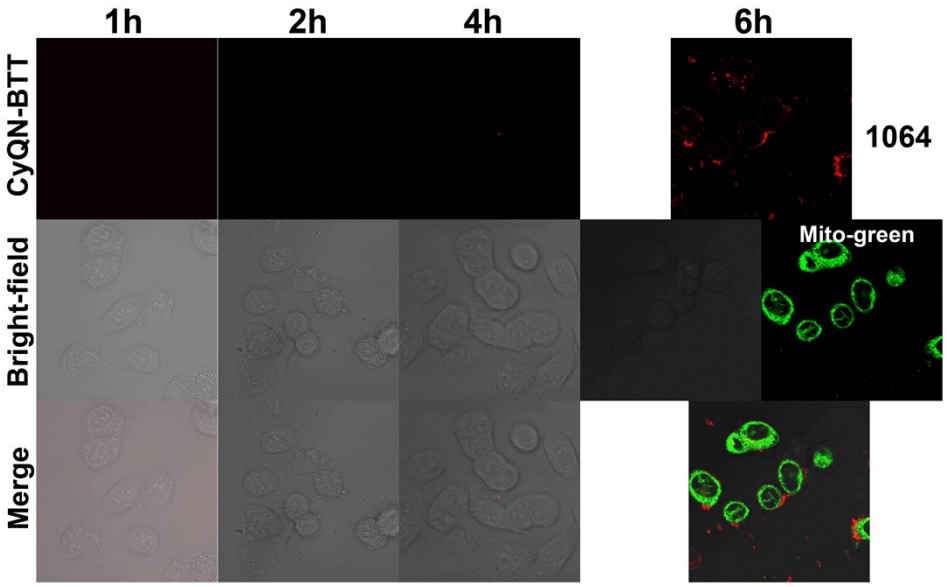

Fig. S33 The intracellular uptake and co-localization CLSM images of CyQN-BTT in 1064 cells. (scale bar: 50.0 μm)

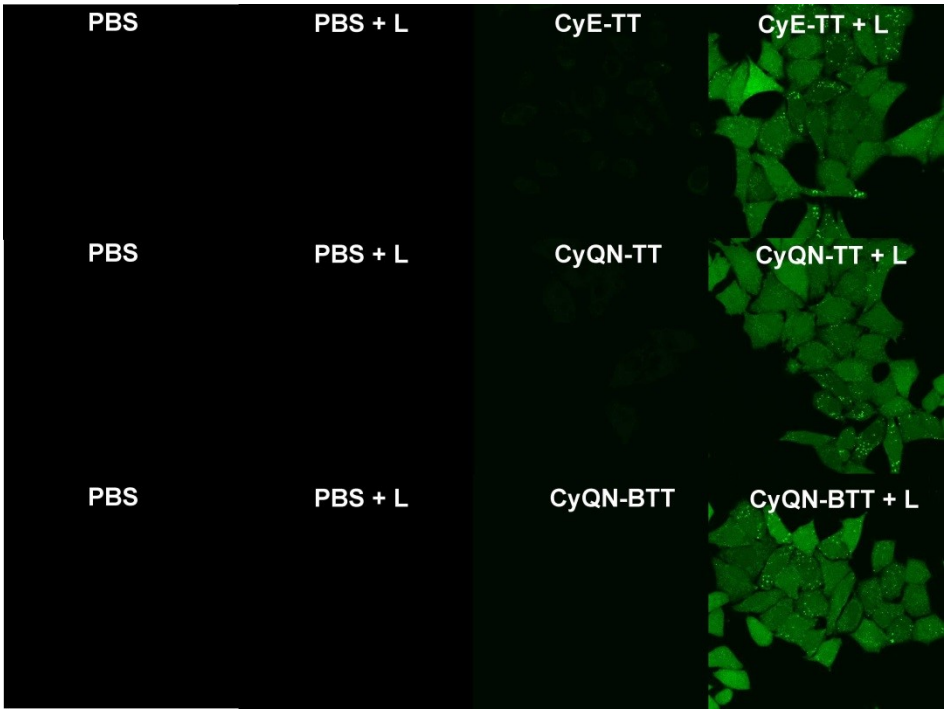

Fig. S34 Intracellular ROS generation of MCF-7 cells with DCFH-DA as indicator. (scale bar: 20.0 μm)

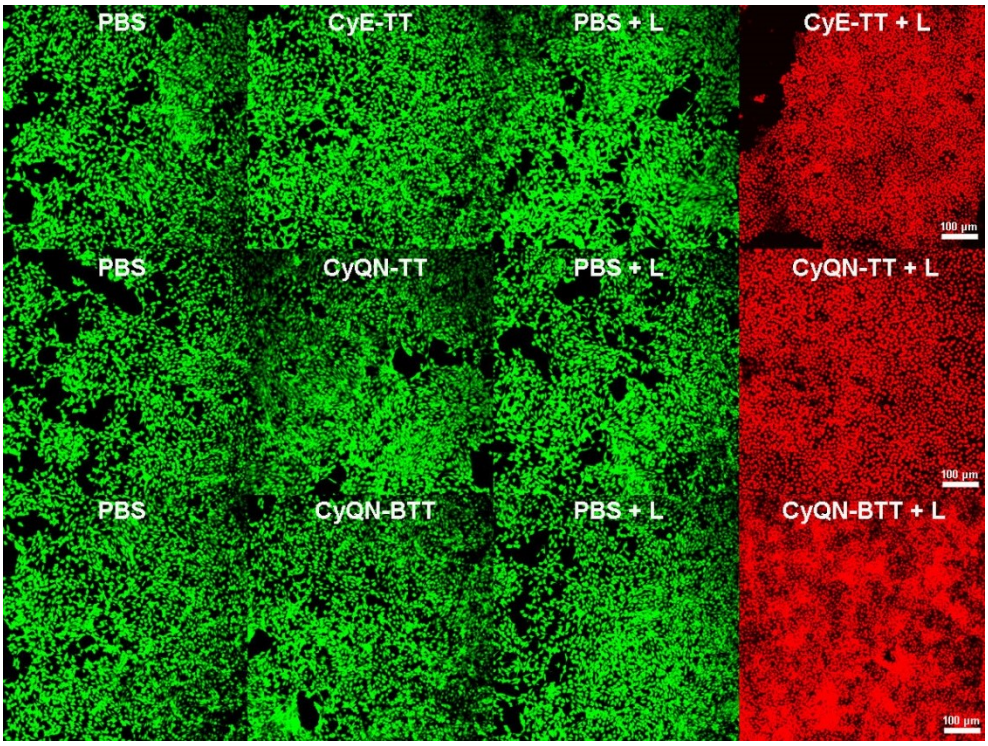

Fig. S35 The live/dead cell staining of 4T1 cells. (scale bar: 100 μm)

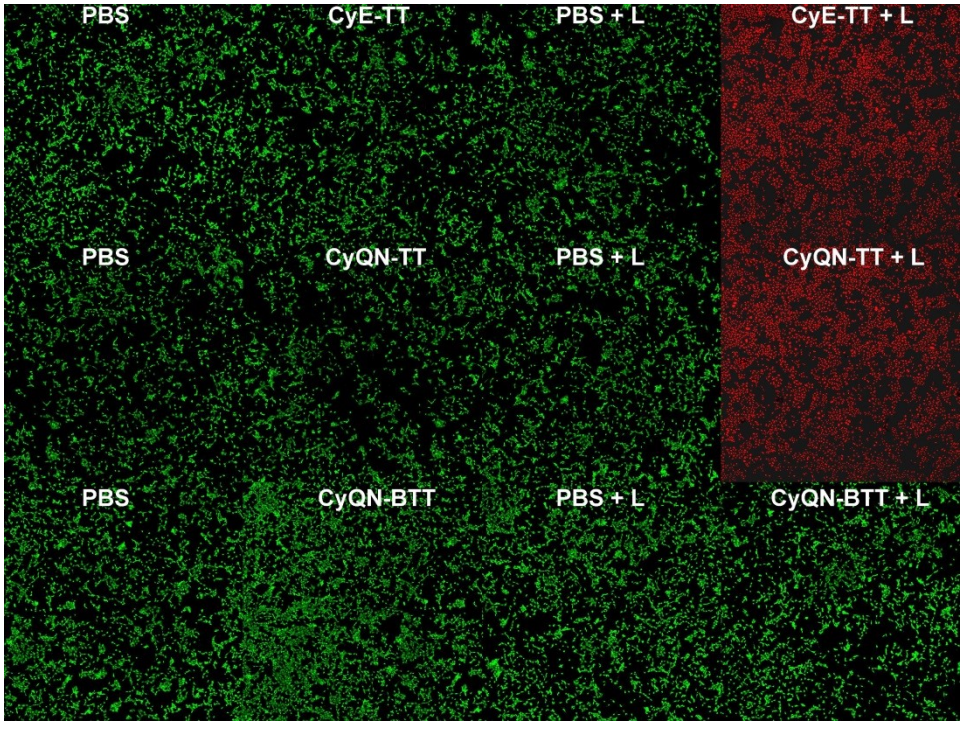

Fig. S36 The live/dead cell staining of 3T3 cells. (scale bar: 100 μm)

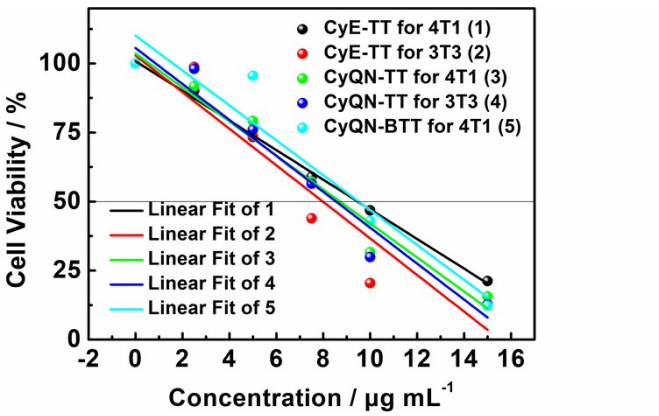

Fig. S37 (1)CyE-TT for 4T1, (2) CyE-TT for 3T3, (3) CyQN-TT for 4T1, (4) CyQN-TT for 3T3, (5) CyQN-B-TT for 4T1.

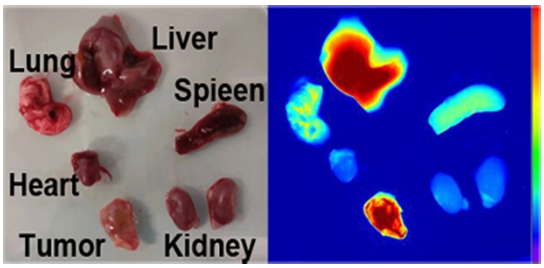

Fig. S38 Fluorescence imaging of major isolated organs and tumor.

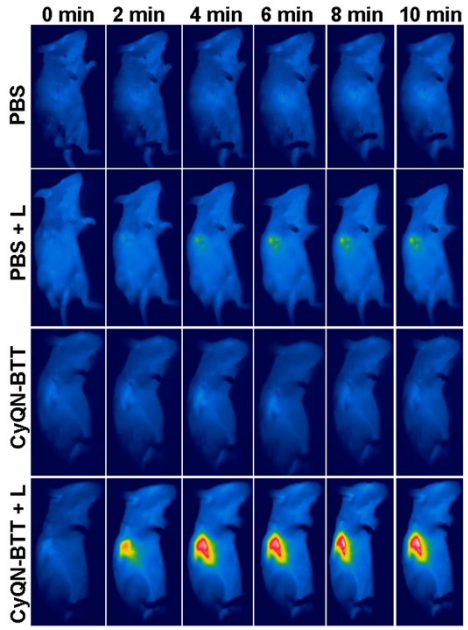

Fig. S39 Infrared thermal images of 4T1-tumor-bearing nude mice after various treatments

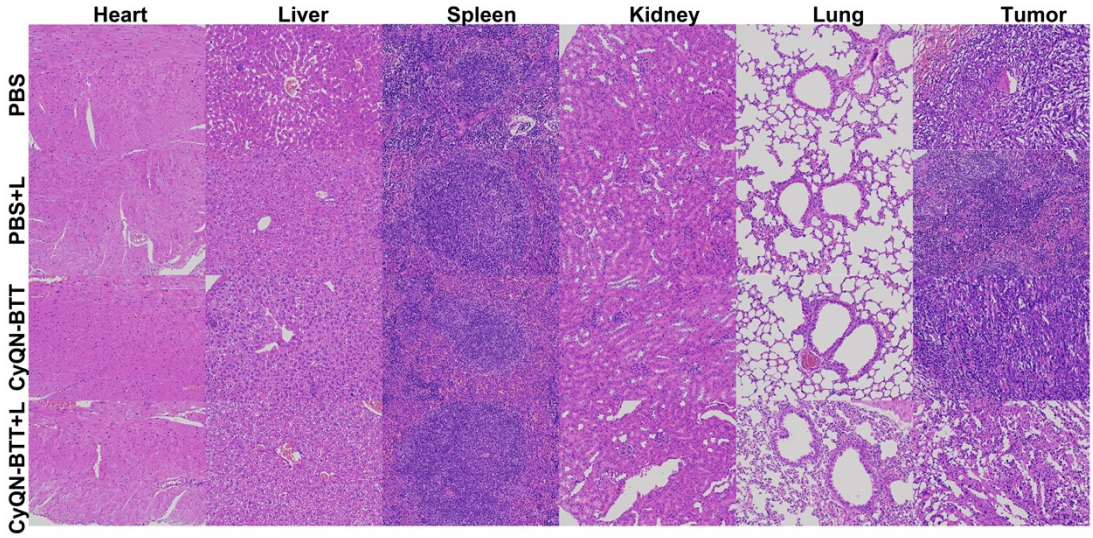

Fig. S40 H&E staining of the major organs and tumors dissected from mice at 10 day after various treatments. Scale bar: 200 μm.

Table S1 FT-IR Absorption peak assignment of CyE-TT, CyQN-TT, and CyQN-BTT.

Peak (cm^{-1})			Assignment
CyE-TT	CyQN-TT	CyQN-BTT	
	3025-3029		C-H bonds vibration of thiophene
	2890-3025		C-H bonds in methyl on triphenylamine
	2300-2884		Bonds vibration of N-C on quaternary ammonium salt
	1650-1762		C=N bonds vibration
	1052-1639		Stretching vibration of C=C bonds on benzene rings
	679-880		Bonds vibration of H-C on benzene

Table S2 The absolute fluorescence quantum yield of CyE-TT, CyQN-TT, and CyQN-BTT, using Absolute quantum yield tester (Hamamatsu Photonics, C11347-11, Japan).

AIEgens	ϕ in DMSO	ϕ in toluene	ϕ in PBS
CyE-TT	0.5 %	14.5 %	14.4 %
CyQN-TT	0.3 %	13.9 %	13.4 %
CyQN-BTT	0.12 %	4.6 %	4.2 %

Table S3 The DFT of CyE-TT, CyQN-TT, and CyQN-BTT in MeOH.

(M062X/TZVP)

AIEgens	GS-opt-geom HOMO / eV	GS-opt-geom LUMO / eV	S1-tdopt-geom S1 / eV	T1-GS-opt-geom T1 / eV	eV/kcal/mol
CyE-TT	-6.47	-2.83	2.0091	1.0672	0.94/21.67
CyQN-TT	-6.53	-2.96	2.0200	1.0743	0.95/21.81
CyQN-BTT	-6.24	-3.42	1.3376	0.8535	0.48/11.16

References

[1] H. Gu, W. J. Liu, S. J. Zhen, S. R. Long, W. Sun, J. F. Cao, X. Z. Zhao, J. J. Du, J. L. Fan, X. J. Peng, ACS Appl. Mater. Interfaces **2021**, 13, 46353-46360.